

## Modeling and optimizing the effect of reverse osmosis membrane separation of biogas slurry using uniform design and response surface methodology

Qizhou Dai, Zonglian Qiu, Tianxiang Zheng, Jianmeng Chen\*

College of Environment, Zhejiang University of Technology, Hangzhou 310032, China, Tel. +86-571-88320276;  
emails: jchen@zjut.edu.cn (J. Chen), dqz@zjut.edu.cn (Q. Dai), 1076608935@qq.com (Z. Qiu), 1036245179@qq.com (T. Zheng)

Received 3 November 2018; Accepted 25 February 2019

---

### ABSTRACT

In recent years, reverse osmosis (RO) membrane technology has been applied to the recovery of biogas slurry and how to improve the performance of RO membrane is becoming important. In this article, response surface methodology (RSM) coupled with uniform design (UD) was applied in RO process. The removal effect of RO process on chemical oxygen demand (COD) of biogas slurry was optimized and a model was setup based on RSM and UD. Verification tests showed satisfactory agreement between the test results and predicted values. In the verification tests, the experimental value of the COD removal rate was 95.54% with satisfied relative error between the predicted value and the experimental result. The results showed that integrating UD and RSM is an effective strategy for optimizing the separation effect of RO process. It is hopeful that this optimization method would play an important role in engineering fields and have a broad application prospect in future.

*Keywords:* Biogas slurry; Optimization; Reverse osmosis; Response surface methodology; Uniform design

---

### 1. Introduction

With the increase in food requirement throughout the world, the scale of livestock sector is increasing day by day, which brings about severe environmental issues caused by the discharge of manure without suitable treatment [1]. Under this background, anaerobic digestion is widely used as an economical option on manure management, because it could not only solve the environmental problem of excess raw manure but also enable livestock farms to maintain the self-sustainment in electricity and heat supply [2,3]. However, the fermentation residues such as the production of biogas slurry have increased significantly with the large-scale development of anaerobic digestion process. The biogas slurry contains organic matters and ammonia nitrogen, which leads to eutrophication and hypoxia. Therefore, how to properly dispose of biogas slurry has become a bottleneck problem restricting the development of anaerobic fermentation technology.

To solve the problem of wastewater pollution and energy conversion, technologies have developed focusing on organics removal, water reuse, nutrient removal, recovery and reuse, such as biological treatment [4], chemical and physical treatment [5,6]. In recent years, due to the shortage of environmental resources, the call for recycling biogas slurry is getting higher and higher and the biogas slurry is often reused for irrigation and as a fertilizer [7]. Under this circumstance, reverse osmosis (RO) membrane technology is gradually being used because it could increase the concentration of manure nutrients and decrease the volume of biogas slurry (due to its excellent interception ability) so that it could be converted into fertilizers better in agricultural field [8]. However, while we are focusing on the recycling of biogas slurry, the effluent quality after RO process should not be ignored. In areas where water-shortage problems are encountered, product water reuse would be especially beneficial for the large pig farms [9]. Therefore, how to obtain high-quality water production is extremely important for the application of RO membrane technology in biogas slurry

---

\* Corresponding author.

reuse. A proper optimization for the separation performance of RO membrane becomes more and more important.

The response surface methodology (RSM) is highly beneficial for clarifying interactions between dependent variables. It could also generate optimal result with balanced conditions and display graphically the relationship of reaction process. Central composite design (CCD) and Box–Behnken design (BBD) are the two conventional experimental designs generally used in RSM [10,11]. However, the use of these two methods is still limited for multi-level tests. It is usually time-consuming to narrow the test range by the steepest climbing test. When using the CCD to optimize the three-factor, four-factor, and five-factor test, the test points could reach 20, 30, and 50, respectively. The corresponding test number of BBD could reach 17, 29, and 46, respectively.

To overcome this shortcoming, the combination of uniform design (UD) and RSM appeared. UD was jointly proposed by Fang and Wang based on quasi-Monte Carlo method in 1978. It combines number-theoretic methods and multivariate statistics methods, which arranges smaller number of experiments by the uniform distribution of test points [12]. It is especially suitable for multi-factors or multi-levels tests when the number of tests is desired to be relatively smaller. In recent years, the combination of RSM and UD acted as an effective optimization method was applied widely to chemistry, metallurgical industry and other fields [13–15].

This study presents a method for optimizing the effluent quality of RO process. The chemical oxygen demand (COD) removal rate was selected as the optimization objective. The RSM improved by UD was used to model and optimize the removal performance. This optimization strategy is expected to play an important role in separation techniques.

## 2. Materials and methods

### 2.1. Water quality analysis

The biogas slurry used in this study was collected from digester on a typical farrow-to-finish swine operation in Fuyang, Zhejiang province, China. The biogas slurry was

pretreated by precipitation and UF before RO process. Specific water quality analysis is shown in Table 1 according to Chinese standard analytical method [16–19]. In addition, materials (analytical grade type) such as NaOH and HCl were purchased from Xilong Scientific Company (Shantou, China).

### 2.2. Experimental setup and materials

A membrane system equipped with UF/RO was applied in this study, as shown in Fig. 1. The wastewater was first pretreated by precipitation module. UF process was stopped when biogas slurry in the beaker reaches to 1,000 mL. Then, the pH of biogas slurry in the beaker was adjusted by 1 M HCl and NaOH solution. Finally, the biogas slurry was pumped to RO module. The concentrate refluxes and circulation until cross-membrane flux is stable, the product water was collected for detection. In the experiment, the precipitation and UF were used to pretreat the wastewater and the pretreatment could effectively remove larger particulates and suspended solids of biogas slurry.

The hollow fiber UF membrane was provided by SaiTe membrane Technology Company (Hangzhou, China). The UF membrane is made of polyvinylidene fluoride, and the pore size of membrane is 0.01  $\mu\text{m}$ . The RO membrane module is BW60 1812-75 aromatic polyamide composite membrane elements manufactured by Dow Chemical Company (Midland, USA). Applying this RO membrane, the higher water flux and higher salt rejection rate could be achieved

Table 1  
Main characteristics of biogas slurry fed to RO membrane system

Chemical oxygen demand, $\text{mg L}^{-1}$	2,590.83
$\text{NH}_3\text{-N}$ , $\text{mg L}^{-1}$	1,355.69
Total nitrogen, $\text{mg L}^{-1}$	1,765.30
Total phosphorus, $\text{mg L}^{-1}$	13.37
Electrical conductivity, $\text{ms cm}^{-1}$	13.37
pH	8.20

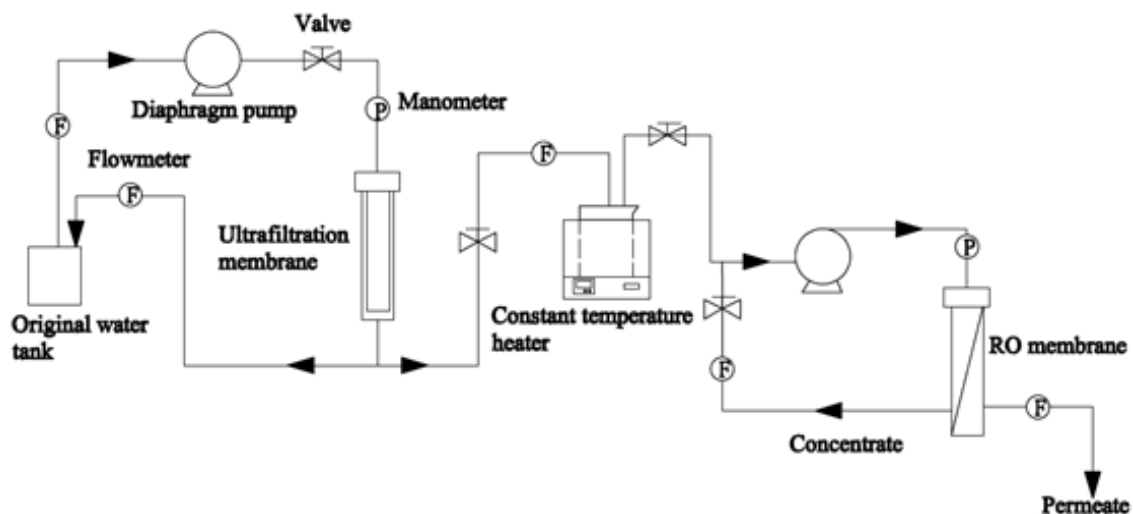


Fig. 1. Schematic diagram of the laboratory scale UF/RO membrane pilot.

under the condition of ultra-low operating pressure. The polyamide film material is resistant to alkali and acid and it has good hydrophilic and mechanical strength and it has high membrane flux and low molecular weight retention.

### 2.3. Experimental and analytical method

Firstly, the pH value of biogas slurry pretreated by UF is adjusted by HCl and NaOH solution. Then, the biogas slurry was adjusted to specified temperature by thermostatic water bath before RO filtration. Finally, the concentration of COD was detected by the spectrophotometer (HACH, DR6000, USA) according to the fast digestion spectrophotometric method [16]. The separation rate of COD was calculated in Eq. (1):

$$R = \frac{C_0 - C_p}{C_0} \times 100\% \quad (1)$$

where  $R$  (%) is the separation rate,  $C_0$  (mg L<sup>-1</sup>) is the concentration of COD of biogas slurry before RO process and  $C_p$  (mg L<sup>-1</sup>) is the concentration of COD in the effluent of RO process.

## 3. Analysis and discussion

The operating pressure, influent pH and influent temperature were selected as the control parameters in this experiment. The whole optimization process is divided into equation fitting, response surface optimization and verification tests.

### 3.1. Experimental design

The range of these main experimental parameters is listed in Table 2, which is based on the practical requirements and the laboratory equipment conditions. The influent pH ranged from 4.0 to 9.5, the operating pressure ranged from 0.5 to 1.0 MPa and the influent temperature ranged from 15.0°C to 35.0°C.

A UD table of mixing level is carried out according to the Table 3, then, the actual parameters and results are listed in Table 4. The  $L_2$ -discrepancy is index to evaluate the uniformity of UD, and it is desirable for obtaining smaller  $L_2$ -discrepancy. In this article, the  $L_2$ -discrepancy of UD table is 0.0433.

### 3.2. Equation fitting

Stepwise regression and partial least squares are favorable methods to fit the results obtained from the UD

Table 2  
Experimental range of uniform design

Parameter	Parameter range
Influent pH	[4.00,9.50]
Operating pressure, MPa	[0.5,1.0]
Influent temperature, °C	[15.0,35.0]

Table 3  
Uniform design with mixed level  $U_{12} (12 \times 6^2)$

Exp. no.	Coded variable levels		
	$X_1$	$X_2$	$X_3$
1	11	6	2
2	3	1	4
3	12	3	5
4	8	2	1
5	6	5	3
6	2	6	5
7	5	2	6
8	4	4	1
9	7	5	4
10	9	4	6
11	1	3	2
12	10	1	3

Table 4  
Experimental results according to uniform design table

Exp. no.	$X_1$	$X_2$	$X_3$	Y
1	9	1	19	95.07
2	5	0.5	27	78.21
3	9.5	0.7	31	90.27
4	7.5	0.6	15	89.04
5	6.5	0.9	23	90.96
6	4.5	1	31	78.07
7	6	0.6	35	80.68
8	5.5	0.8	15	88.63
9	7	0.9	27	92.60
10	8	0.8	35	92.19
11	4	0.7	19	78.49
12	8.5	0.5	23	90.55

according previous research [20,21]. In this article, the progress of model fitting was achieved using DPS7.05 software. Then, linear and quadratic polynomial equations of stepwise regression and partial least squares were built to describe the relationship between the experimental parameters and separation rate of COD. Finally, in order to judge the quality of these models, the diagnostic criteria of multivariate regression was performed [22].

The detailed statistical analysis of models is listed in Table 5, where  $R^2$  is the determinate coefficient, which is specified as the ratio of the described variable to the total variation and the degree of fitness of the model;  $F$ -value is a statistic originated from the Fischer test that displays whether the data departs significantly from the mean. The regression model is acceptable when the  $F$ -value of the result is greater than critical  $F$ -values (at a certain level of significance expressed as alpha; in this article, the value of alpha is 0.05). The  $p$ -value is probability of differences between samples probability due to sampling errors. Specifically, if a  $p$ -value

Table 5  
Regression models of stepwise regression and partial least squares for the separation rate of COD

No.	Fitting method	Fitting model	$R^2$	$F$ -value	$p$ value	Critical $F$ -value
(1)	linear stepwise regression	$Y = 64.8358 + 2.9565X_1 + 10.7829X_2 - 0.2327X_3$	0.8431	14.3324	0.0014	4.07
(2)	quadratic polynomial stepwise regression	$Y = 43.5540 + 10.5489X_1 - 0.9066X_1^2 - 0.0224X_3^2 + 1.7165X_1X_2 + 0.1337X_1X_3$	0.9797	58.1537	0.0001	4.39
(3)	Linear model of partial least squares	$Y = 63.2632 + 2.9781X_1 + 11.1058X_2 - 0.1852X_3$	0.8401	–	–	–
(4)	Quadratic polynomial model of partial least squares	$Y = 21.2704 + 8.7879X_1 + 72.8229X_2 + 0.0349X_3 - 0.6229X_1^2 - 36.5459X_2^2 + 0.0008X_3^2 + 1.6846X_1X_2 + 0.0468X_1X_3 - 0.7556X_2X_3$	0.9204	–	–	–

Note:  $Y$  is the separation rate of COD.  $X_1$ ,  $X_2$  and  $X_3$  represent the influent pH, the operating pressure and the influent temperature, respectively.

is smaller than 0.05, the models would fit the experimental results well.

As shown in Table 5, model (2) has highest determinate coefficient  $R^2$  among four models, which displayed favorable fitness. In addition, the  $F$ -value (58.15) of model (2) was greater than critical  $F$ -value ( $F_{0.05}(5,6) = 4.39$ ), which proves that this equation is highly significant. In addition, the  $p$ -value of model (2) is only 0.0001, which further demonstrates the good fitness of model (2). Therefore, the best model was as follows (introduce and reject insignificant variables at the confidence level of  $\alpha = 0.10$ ):

$$Y = 43.5540 + 10.5489X_1 - 0.9066X_1^2 - 0.0224X_3^2 + 1.7165X_1X_2 + 0.1337X_1X_3 \quad (2)$$

where  $Y$  is the separation rate of COD;  $X_1$ ,  $X_2$  and  $X_3$  represent the influent pH, operating pressure and the influent temperature, respectively.

The relationship of experimental values and predicted values based on the model (2) is shown graphically in Fig. 2. The predicted values were generated after calculating using model (2). As depicted in Fig. 2, most points distributed

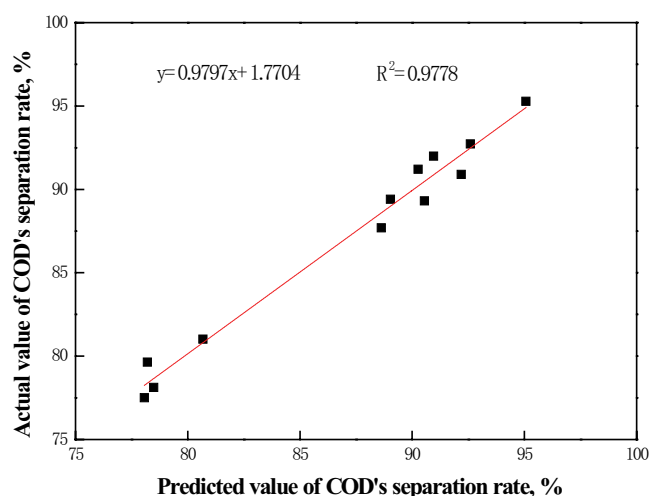


Fig. 2. Predicted and actual separation rate of COD.

near to the straight line where the measured and predicted removal efficiencies are similar, indicating further that the regression equation fits the experimental results well.

### 3.3. Analysis of response surface

Through significance analysis, the quadratic polynomial model of stepwise regression had been selected. However, it is hard to predict intuitively the separation performance by model (2), because that there is a complex nonlinear relationship in this equation. Based on the quadratic polynomial model of stepwise regression, one independent variable was controlled at middle level when the other independent variables were adjusted from the lowest to the highest level. Then, the interaction between experimental parameters and the separation rate of COD was investigated as illustrated in Figs. 3a–d.

In Figs. 3a and b, the degree of growth for separation rate of COD is low when the influent pH is less than 7. Higher COD rejection rate could be achieved when influent pH is relatively high. On the other hand, the higher the operating pressure, the better the COD removal rate obtained. Also, the degree of COD removal rate could be enhanced when the influent pH is between 6.0 and 8.5. This shows that the COD rejection rate is more affected by influent pH. In addition, as illustrated in Figs. 3c and d, the influent temperature has a strong influence on the COD rejection rate when the influent pH is less than 6, and the COD rejection rate decreased as the influent temperature increased. The COD rejection rate could be maintained at a higher level regardless of the influent temperature when the influent pH is greater than 6.

In order to achieve a better explanation of the relationship between COD removal rate and investigated variables, the effect of single factor on the COD removal rate was explored.  $X_1$ ,  $X_2$  and  $X_3$  in Eq. (2) were adjusted as follows: two of the three influencing factors are controlled to a medium level, while the other influencing factor is changed within the operating range. Through the above adjustment, the respective effect of three influencing factors on COD separation rate was observed separately (presented in Figs. 4a–c).

Fig. 4a presents the effect of operating pressure on COD separation rate. As could be seen, the separation rate of COD increased from 87.12% to 92.70% with the operating pressure increased. According to dissolution diffusion model,

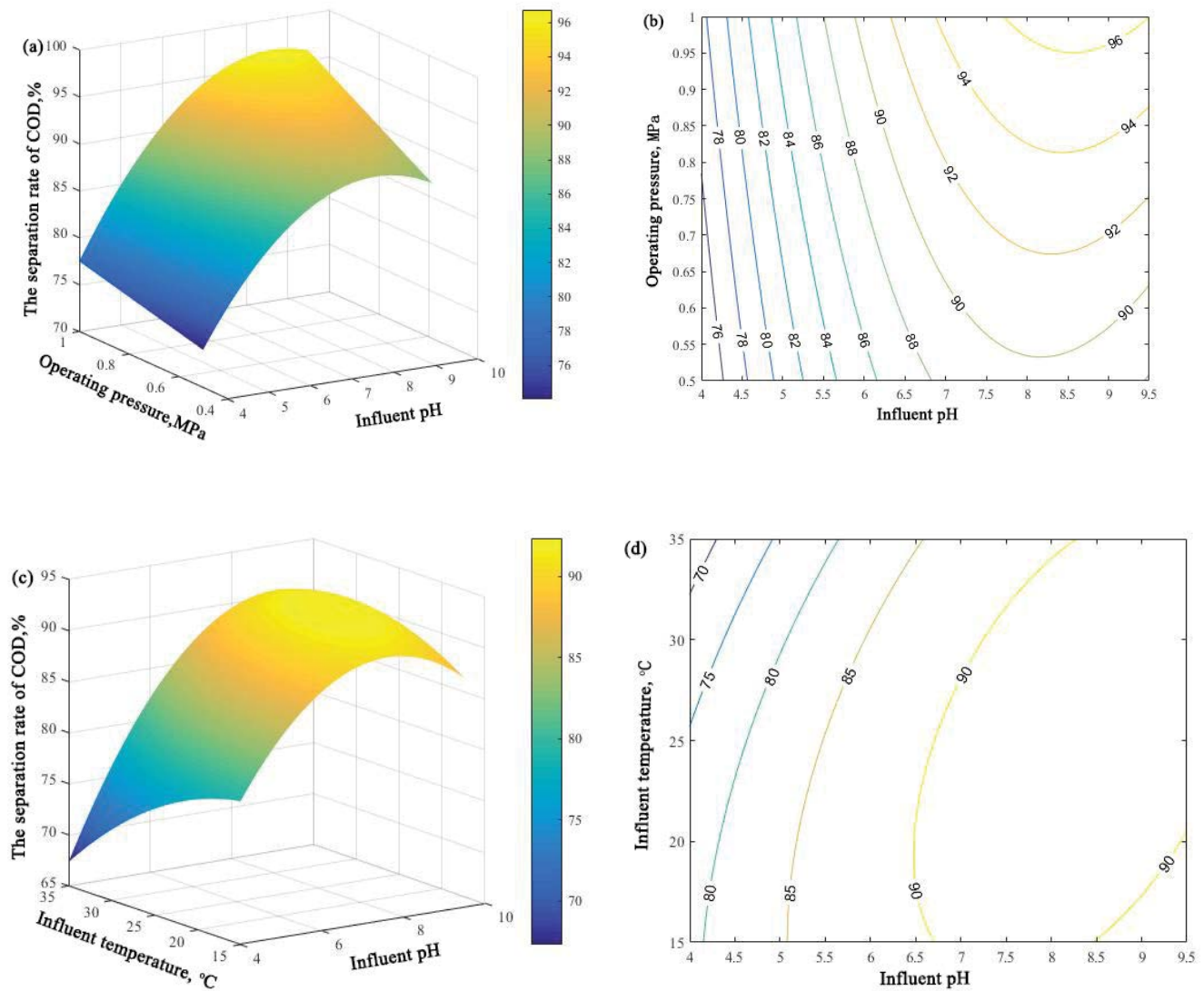


Fig. 3. Response surface plots and contours for interactions of investigated parameters. (a) and (b) reflect the interaction between operating pressure and the influent pH; (c) and (d) reflect the interaction between the influent temperature and the influent pH.

the solvent flux depends on the pressure difference [23,24]. The solvent flux will increase and the solute flux will stay the same with operating pressure increased, which results in the increase of removal rate of solute. Fig. 4b presents the effect of the influent pH on COD separation rate, it showed a trend of rising first and then declining. This could be attributed to the dissociation of organic acids [25]. The organic acid will be unionized at lower pH, and will pass more readily through membrane pores. As the pH increases, the organic acid will be dissociated, and then most of the dissociated acid is retained due to its mutual repulsion with the membrane [26,27]. The concentrates of the membrane could be further treated by advanced oxidation, such as electrochemical oxidation [28–29]. The decrease in the retention rate at pH 9.5 may be due to membrane fouling caused by inorganic salt deposition with pH increased, which leads to a decrease in the rejection rate. Fig. 4c presents the effect of the influent

temperature on COD separation rate. As can be seen, the separation rate of COD maintained relative stability before 20°C, and it showed sharp decline after 20°C.

### 3.4. Verification

The optimum conditions and the optimal value were generated by data processing system according to the results of UD. Optimum conditions and optimal value are given in Table 6. For the purpose of verifying the validity of optimal results, three parallel tests are carried out based on the optimal condition. According to the accuracy of experimental equipment and measuring instrument, the optimum conditions were adjusted appropriately in verification tests. The result indicated that the separation rate of COD (96.41%) predicted in optimum conditions was close to the mean value of three verification tests (95.54%).

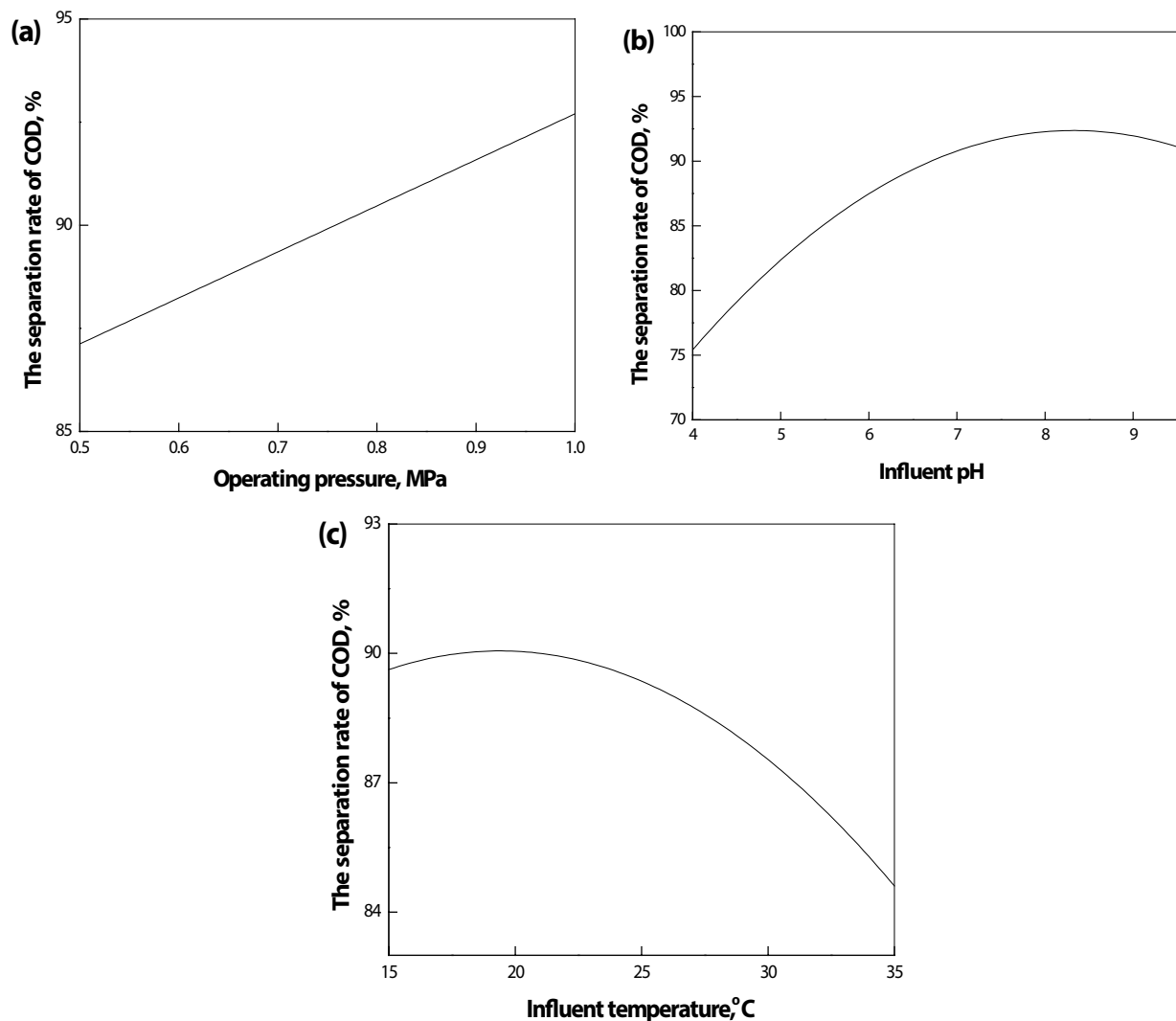


Fig. 4. Respective effect of three influencing factors on COD separation rate, (a) operating pressure; (b) influent pH; (c) influent temperature.

Table 6  
Results of predicted and experimental result at optimum conditions

	$X_1$	$X_2$ , MPa	$X_3$ , °C	$R_{\text{COD}}$ , %
Optimal value	8.0631	1.0	25.7910	96.41
Actual value	8.1	1.0	25.8	95.54

#### 4. Conclusion

In this article, the RSM coupled with UD was applied to model and optimize the COD removal rate. According to the experimental results, the influent pH and operating pressure ( $X_1, X_2$ ), the influent pH and the influent temperature ( $X_1, X_3$ ) had interactive effects on the COD separation rate. Thus, we focused the combined choice for the influent pH, operating pressure and the influent temperature in RO separation process. The optimal conditions for COD separation rate were the influent pH of 8.1, operating pressure of 1 MPa and the

influent temperature of 25.8°C. Under this operating condition, the predicted optimal value of COD removal rate reached is 96.41%. The actual separation rate of COD was 95.54%, which was in agreement with the predicted result. In conclusion, the combination of the UD and RSM is an effective and powerful approach for the optimization of RO process for biogas slurry treatment. This paper could provide basic data and technique reference in engineering fields and have a broad application prospect in future.

#### Acknowledgment

The authors are grateful for the financial support provided by the Project of Science and Technology Department of Zhejiang Province (2015C03017).

#### References

- [1] F. Montes, R. Meinen, C. Dell, A. Rotz, A.N. Hristov, J. Oh, G. Waghorn, P.J. Gerber, B. Henderson, H.P.S. Makkar,

- J. Dijkstra, SPECIAL TOPICS — Mitigation of methane and nitrous oxide emissions from animal operations: II. A review of manure management mitigation options, *J. Anim. Sci.*, 91 (2013) 5070–5094.
- [2] S.V.W.B. de Oliveira, A.B. Leoneti, G.M.M. Caldo, M.M.B. de Oliveira, Generation of bioenergy and biofertilizer on a sustainable rural property, *Biomass Bioenergy*, 35 (2011) 2608–2618.
- [3] H. Insam, I.H. Franke-Whittle, S.M. Podmirseg, Agricultural waste management in Europe, with an emphasis on anaerobic digestion, *J. Integr. Field Sci.*, 11 (2014) 13–17.
- [4] X. Chen, G. Li, H. Lin, Y. Li, Y. Ma, R. Dai, J. Zhang, Operation performance and membrane fouling of a spiral symmetry stream anaerobic membrane bioreactor supplemented with biogas aeration, *J. Membr. Sci.*, 539 (2017) 206–212.
- [5] L. Wang, J. Cao, X. Cheng, C. Lei, Q. Dai, B. Yang, Z. Li, M.A. Younis, L. Lei, Y. Hou, K. Ostrikov, ZIF-Derived carbon nanoarchitecture as a bifunctional ph-universal electrocatalyst for energy-efficient hydrogen evolution, *ACS Sustainable Chem. Eng.*, 7 (2019) 10044–10051.
- [6] X. Bian, Y. Xia, T. Zhan, L. Wang, W. Zhou, Q. Dai, J. Chen, Electrochemical removal of amoxicillin using a Cu doped PbO<sub>2</sub> electrode: Electrode characterization, operational parameters optimization and degradation mechanism, *Chemosphere*, 233 (2019) 762–770.
- [7] Z. Liu, K. Sun, B. Zheng, Q.L. Dong, G. Li, H. Han, Z. Li, T. Ning, Impacts of straw, biogas slurry, manure and mineral fertilizer applications on several biochemical properties and crop yield in a wheat-maize cropping system, *Plant Soil Environ.*, 65 (2019) 1–8.
- [8] C. Ledda, A. Schievano, S. Salati, F. Adani, Nitrogen and water recovery from animal slurries by a new integrated ultrafiltration, reverse osmosis and cold stripping process: a case study, *Water Res.*, 47 (2013) 6157–6166.
- [9] L. Masse, D.I. Masse, Y. Pellerin, The use of membranes for the treatment of manure: a critical literature review, *Biosyst. Eng.*, 98 (2007) 371–380.
- [10] N.F. Razali, A.W. Mohammad, N. Hilal, C.P. Leo, J. Alam, Optimisation of polyethersulfone/polyaniline blended membranes using response surface methodology approach, *Desalination*, 311 (2013) 182–191.
- [11] K.W. Jung, M.J. Hwang, M.J. Cha, K.H. Ahn, Application and optimization of electric field-assisted ultrasonication for disintegration of waste activated sludge using response surface methodology with a Box–Behnken design, *Ultrason. Sonochem.*, 22 (2015) 437–445.
- [12] W.H. Chan, S.C. Tsao, Fabrication of nanofiltration membranes with tunable separation characteristics using methods of uniform design and regression analysis, *Chemom. Intell. Lab. Syst.*, 65 (2003) 241–256.
- [13] D.H. Luo, Optimization of total polysaccharide extraction from *Dioscorea nipponica Makino* using response surface methodology and uniform design, *Carbohydr. Polym.*, 90 (2012) 284–288.
- [14] J.M. Wang, S. Lan, W.K. Li, Numerical simulation and process optimization of an aluminum holding furnace based on response surface methodology and uniform design, *Energy*, 72 (2014) 521–535.
- [15] D.Q. Sun, A.Y. Xue, B. Zhang, X. Xue, J. Zhang, W. Liu, Enhanced oral bioavailability of acetylpuerarin by poly(lactide-co-glycolide) nanoparticles optimized using uniform design combined with response surface methodology, *Drug Des. Dev. Ther.*, 10 (2016) 2029–2039.
- [16] The State Environmental Protection Standards of the People's Republic of China (HJ/T 399-2007): Water Quality-Determination of Chemical Oxygen Demand-Fast Digestion-Spectrophotometric Method [S], China Environmental Science Press, Beijing, 2009.
- [17] The State Environmental Protection Standards of the People's Republic of China (HJ 535-2009): Water Quality-Determination of Ammonia Nitrogen-Nessler Reagent Spectrophotometry [S], China Environmental Science Press, Beijing, 2009.
- [18] The State Environmental Protection Standards of the People's Republic of China (HJ 636-2012): Water Quality-Determination of Total Nitrogen-Alkaline Potassium Persulfate Digestion UV Spectrophotometric Method [S], China Environmental Science Press, Beijing, 2012.
- [19] The State Environmental Protection Standards of the People's Republic of China (GB 11893-89): Water Quality-Determination of Total Phosphorus-Ammonium Molybdate Spectrophotometric Method[S], China Environmental Science Press, Beijing, 1989.
- [20] J.P. Wang, Y.Z. Chen, Y. Wang, S.J. Yuan, H.Q. Yu, Optimization of the coagulation-flocculation process for pulp mill wastewater treatment using a combination of uniform design and response surface methodology, *Water Res.*, 45 (2011) 5633–5640.
- [21] F. Wei, H. Wu, J. Cheng, Y. Liu, G. Zhu, Study on the application of multifactor experimental designs in pesticide microemulsion development, *Chin. J. Pestic. Sci.*, 11 (2009) 373–380.
- [22] W. Jiang, S.Z. Wang, Z.L. Yang, B.S. Fang, B<sub>12</sub>-independent glycerol dehydratase and its reactivase from *Clostridia butyricum*: optimizing cloning by uniform design logic, *Eng. Life Sci.*, 15 (2015) 519–524.
- [23] T.Y. Qiu, P.A. Davies, Concentration polarization model of spiral-wound membrane modules with application to batch-mode RO desalination of brackish water, *Desalination*, 368 (2015) 36–47.
- [24] J.S. Choi, J.T. Kim, Modeling of full-scale reverse osmosis desalination system: Influence of operational parameters, *J. Ind. Eng. Chem.*, 21 (2015) 261–268.
- [25] L. Masse, D.I. Masse, Y. Pellerin, The effect of pH on the separation of manure nutrients with reverse osmosis membranes, *J. Membr. Sci.*, 325 (2008) 914–919.
- [26] P. Fu, H. Ruiz, K. Thompson, C. Spangenberg, Selecting membranes for removing NOM and DBP precursors, *J. Am. Water Works Assn.*, 86 (1994) 55–72.
- [27] T. Matsuura, S. Sourirajan, Physicochemical criteria for reverse osmosis separation of monohydric and polyhydric alcohols in aqueous solutions using porous cellulose acetate membranes, *J. Appl. Polym. Sci.*, 15 (2010) 2905–2927.
- [28] M. Weng, J. Pei, Electrochemical oxidation of reverse osmosis concentrate using a novel electrode: parameter optimization and kinetics study, *Desalination*, 399 (2016) 21–28.
- [29] M. Weng, X. Yu, Electrochemical oxidation of para-aminophenol with rare earth doped lead dioxide electrodes: kinetics modeling and mechanism, *Front. Chem.*, 7 (2019) 382.